

135

Journal of the
IRRIGATION AND DRAINAGE DIVISION
Proceedings of the American Society of Civil Engineers

BORDER IRRIGATION ADVANCE AND EPHEMERAL FLOOD WAVES

By Roger E. Smith,¹ A. M. ASCE

INTRODUCTION

A kinematic wave was described by Lighthill and Whitham (8) as a wave whose properties can be described by an equation of continuity and a stage-discharge relation. This implies that momentum changes are negligible. Reviews of recent applications of the kinematic approximation in open channel hydraulics were given by Woolhiser and Liggett (16) and Kibler and Woolhiser (5). Smith and Woolhiser (11) described the hydrologic response of an elementary watershed by a kinematic wave, using a theoretical solution of porous media flow for an infiltration model. The spatial variation in interaction of surface-subsurface flow was only approximated, however.

Described herein is a method of predicting advance rate, surface profiles, and modifications with time to kinematic wave flow over an initially dry infiltrating plane. Interaction of surface flow and infiltration loss is treated explicitly with point infiltration rate considered to be a function of time since wetting (opportunity time). This technique is applicable for flood wave movement and attenuation in dry alluvial channels such as commonly occur in the Southwestern United States. A special case of this model, where upstream flow is a step function, describes the much studied border irrigation advance problem.

KINEMATIC FLOW ON INITIALLY DRY PLANE

Continuity for unsteady open channel flow in any channel may be expressed as

$$\frac{\partial A}{\partial t} + \frac{\partial (uA)}{\partial x} = pq(x, t) \dots \dots \dots (1a)$$

Note.—Discussion open until November 1, 1972. To extend the closing date one month, a written request must be filed with the Executive Director, ASCE. This paper is part of the copyrighted Journal of the Irrigation and Drainage Division, Proceedings of the American Society of Civil Engineers, Vol. 98, No. IR2, June, 1972. Manuscript was submitted for review for possible publication on December 1, 1971.

¹Research Hydraulic Engr., Southwest Watershed Research Center, Tucson, Ariz.

in which A = channel cross-sectional area; t = time; u = local velocity; x = distance along channel; p = wetted perimeter; and $q(x, t)$ = local inflow (+) or outflow (-) rate. For wide channels or surface flow, the continuity equation is similar:

$$\frac{\partial h}{\partial t} + \frac{\partial (uh)}{\partial x} = q(x, t) \dots\dots\dots (1b)$$

in which h = depth. For simplicity, the following comments will refer only to plane flow.

To complete the kinematic description, the stage-discharge relation:

$$Q = \alpha h^{m+1} \dots\dots\dots (2a)$$

is taken from a laminar flow or a Chezy or Manning turbulent flow friction slope relation, all of which may be expressed as

$$u = \alpha h^m \dots\dots\dots (2b)$$

in which α and m are constant coefficient and exponent parameters, respectively. The Darcy-Weisbach expression can be used to unify friction slope ex-

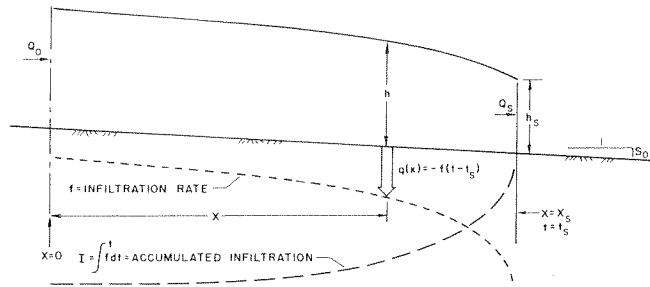


FIG. 1.—DEFINITION SKETCH FOR KINEMATIC SHOCK WAVE ADVANCE ON INFILTRATING PLANE

pressions for laminar and turbulent flow. For laminar flow, m would be 2, and α could be expressed as $C_l S$ in which C_l = a laminar resistance coefficient, and S = slope. Likewise in turbulent flow, m is 1/2 for a Chezy relation and 2/3 for a Manning relation. Then α would be a function of a turbulent resistance coefficient C_t , and \sqrt{S} .

Eqs. 1b and 2b may be combined as

$$\frac{\partial h}{\partial t} + (m + 1) \alpha h^m \frac{\partial h}{\partial x} = q(x, t) \dots\dots\dots (3)$$

Fig. 1 shows the problem to which this kinematic description of surface flow will be applied. A flow of $Q_0(t)$ begins at $x = 0$ at time $t = 0$. The wave front is assumed to travel as a kinematic shock or flow discontinuity (5) which moves with a velocity

$$U_s(x) = \frac{\Delta Q}{\Delta h} \dots\dots\dots (4)$$

in which ΔQ and Δh are change in discharge and depth, respectively, across the

shock. This reduces to Q_s/h_s when the initial depth and flow are zero, as in this case, where h_s and Q_s are depth and flow rate immediately behind the shock. Point infiltration is a function of time since the shock passed the point, and thus is dependent on time and shock velocity.

Although the goodness of the kinematic assumption can be tested by order of magnitude analysis of the terms of the complete energy equations for unsteady flows (4), it is sufficient for this discussion to refer to a nondimensional parameter which Woolhiser and Liggett (16) derived to rate the kinematic assumption for plane response to rainfall:

$$k = \frac{S_o L_o}{H_o F_o^2} \dots \dots \dots (5)$$

in which S_o = plane slope; L_o = plane length; H_o = normal depth for equilibrium flow at the plane outlet; and F_o = normal depth Froude number.

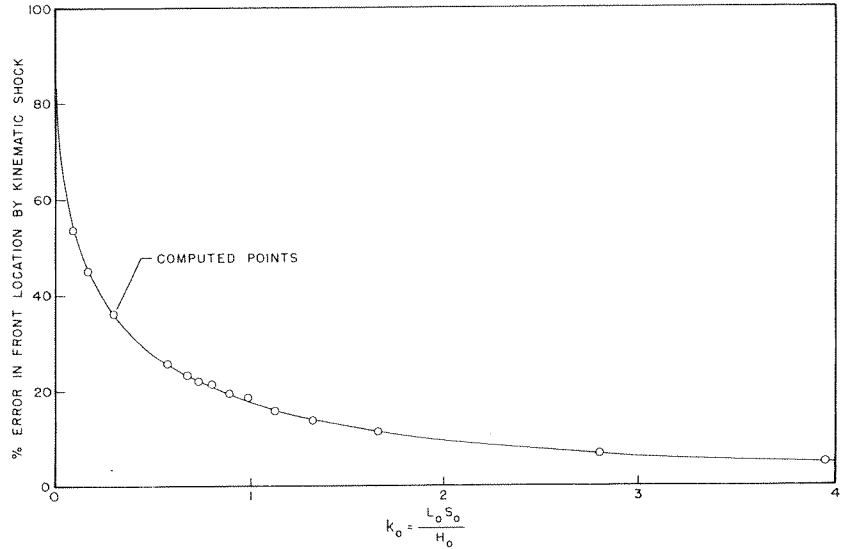


FIG. 2.—ESTIMATED ERROR IN WAVE ADVANCE PREDICTION FROM KINEMATIC SHOCK ASSUMPTION, BASED ON DATA FROM TINNEY AND BASSETT (11)

It can be seen from Fig. 1 that some question arises as to how this parameter should be applied to indicate validity of kinematic assumptions for the present case. The flow described by Fig. 1 is both similar and dissimilar to the overland flow from rainfall on an impervious plane. Term k was derived in the process of normalizing the complete dynamic equations. Similar normalization can be carried out for the case of Fig. 1, but normalizing length should be variable to reflect flow length:

$$L_o = \int_0^t U_s dt \dots \dots \dots (6)$$

in which $t_s(x)$ = time when the shock reaches point x .

Without infiltration, kinematic shock depth equals normal depth, and experimental agreement with such a step wave can indicate goodness of the kinematic assumption for shock movement. Tinney and Bassett (12) performed experiments measuring shock front shape under a few variations in slope, roughness, and flow rate. The normalizing parameter they derived for expression of their results was $S_o L_o / H_o$, here termed k_o , which is remarkably similar to k . From their results, the error in prediction of front location by a kinematic shock can be derived, and Fig. 2 is such a prediction. As would be expected, the kinematic shock has a sizeable error for small values of k_o , but the approximation is quite good for all values of k_o greater than 2 to 3. Momentum change and gravity have their greatest effects at small distances from the front. On the other hand, the kinematic profile cannot be far in error, if continuity is preserved, for long relatively shallow flows. Additional uncertainties arise for description of large flood waves where $Q_o(t)$ varies over a wide range. Woolhiser and Liggett's results indicate good kinematic approximation for $k > 50$ (approximately), and a similar order of approximation should apply for most values of F_o for shock flow, according to Fig. 2, as $k = k_o / F_o^2$. F_o for these data range from 0.22 to 0.95.

POINT INFILTRATION FROM PONDED SURFACE

Work of various investigators (2,9,14), as well as numerical solutions for theoretical equations by the writer (10) indicate that perhaps the best algebraic formula for infiltration from a ponded surface is

$$- q(x) = f(\tau) = K(\tau)^{-a} + f_o \dots \dots \dots (7)$$

in which τ is defined as the time since ponding of the surface; K and a = soil specific constants; and f_o = asymptotic long-time infiltration rate, theoretically equal to saturated conductivity for very deep water tables. This is essentially the Kostiaikov infiltration formula, plus a constant final rate. This equation will be used in this work to describe infiltration at any point $x < x_s$ so that $\tau = t - t_s$ for all $t > t_s$.

SOLUTION BY METHOD OF CHARACTERISTICS

Characteristic Net Construction.—The partial differential Eq. 3 can be reduced to two ordinary differential equations in x , t , and h , known as characteristic equations (16):

$$\frac{dx}{dt} = \beta h^m \dots \dots \dots (8)$$

in which $\beta = (m + 1) \alpha$, and

$$\frac{dh}{dt} = q = - f(\tau) \dots \dots \dots (9)$$

In addition, from Eq. 4 shock velocity can be specified as

$$U_s = \alpha h_s^m = \frac{dx_s}{dt} \dots \dots \dots (10)$$

The basis of the method of solution by characteristics was suggested in a discussion by Woolhiser (15) of a paper by Chen (1). The characteristic solution in the x, t plane is shown in Fig. 3.

Construction of the characteristic path proceeds from the upstream boundary, where $Q_o(t)$ is specified, to the shock and forward in time. Two cases in the solution for new points on the characteristic surface arise: one for extension of characteristics behind and independent of the shock, and another

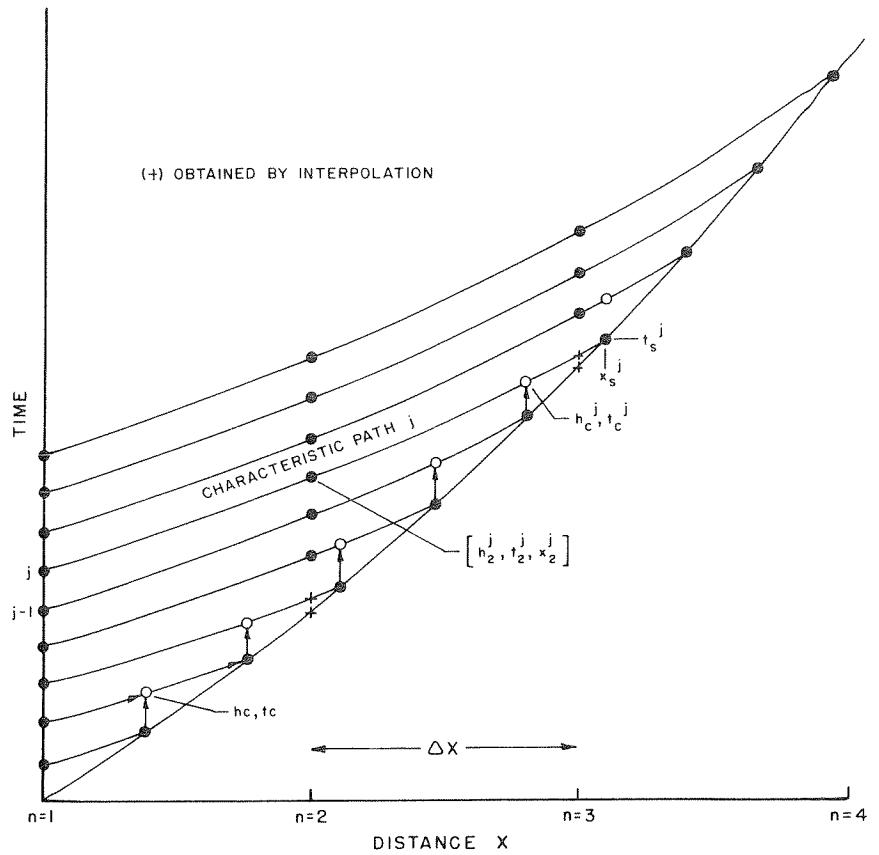


FIG. 3.—DEFINITION SKETCH FOR GRID CONSTRUCTION FOR SOLUTION OF WAVE ADVANCE BY METHOD OF CHARACTERISTICS

for location of an intersection of a characteristic and the new shock location. The first case requires simultaneous solution of two equations (Eqs. 8 and 9), and the latter requires three equations (Eqs. 8, 9, and 10). For simple characteristic extension, either Δx or Δt may be specified. For this problem, Δx increments are specified.

First consider simple extension of a characteristic across a given Δx from point n to $n + 1$ in which $x = (n - 1) \Delta x$. Eqs. 8 and 9 may be rewritten as

follows, using superscripts to indicate characteristic number and subscripts for distance. From Eq. 8

$$\frac{x_{n+1} - x_n}{t_{n+1} - t_n^j} = \frac{\beta}{2} [(h_n^j)^m + (h_{n+1}^j)^m] \dots \dots \dots (11)$$

and from Eq. 9

$$\frac{h_{n+1}^j - h_n^j}{t_{n+1}^j - t_n^j} = - \bar{f} [\tau_n^j, \tau_{n+1}^j] \dots \dots \dots (12)$$

in which $\bar{f}(\tau_1, \tau_2) = \frac{1}{\tau_2 - \tau_1} \int_{\tau_1}^{\tau_2} f(t) dt \dots \dots \dots (13)$

Eqs. 11 and 12 are reduced to one equation in h_{n+1}^j which is solved by Newton iteration. For $f(t)$ as defined by Eq. 7, ($0 < a < 1$) Eq. 13 becomes

$$\bar{f}(\tau_1, \tau_2) = f_0 + \left(\frac{K}{1-a} \right) \left(\frac{\tau_2^{1-a} - \tau_1^{1-a}}{\tau_2 - \tau_1} \right) \dots \dots \dots (14)$$

Definition of shock movement is somewhat more complicated; first, referring to Fig. 3, the point h_c^j, t_c^j is defined for the location x_s^{j-1} by the technique defined previously, moving along the characteristic from the last net point behind the shock. Then, information at point h_c, t_c and x_s^{j-1}, t_s^{j-1} , and h_s^{j-1} is used in finite difference forms of Eqs. 8-10:

$$\frac{x_s^j - x_s^{j-1}}{t_s^j - t_c^j} = \frac{\beta}{2} [(h_s^j)^m + (h_c^j)^m] \dots \dots \dots (15)$$

$$\frac{h_s^j - h_c^j}{t_s^j - t_c^j} = - \bar{f}(t_c^j, 0) \dots \dots \dots (16)$$

and from Eq. 10:

$$\frac{x_s^j - x_s^{j-1}}{t_s^j - t_s^{j-1}} = \frac{\alpha}{2} [(h_s^j)^m + (h_s^{j-1})^m] \dots \dots \dots (17)$$

This system of equations is reduced to one equation in h_s^j by algebraic substitution, and this implicit equation is solved by Newton iteration. Although the system could equally well be solved for t_s^j , it was found that solution in h_s^j provided superior convergence properties and therefore speed of solution. Terms t_s^j and x_s^j are then found by back substitution.

Computation Procedure.—The characteristic net may be extended to a specified limit in both x and t . Intersection of the shock front with an x limit (x_L) does not affect solutions for $t > t_s(x_L)$. To define accurately the shock path between x grid points, t at $x = 0$ is chosen so that the shock location x_s^j is found for $2 \leq j \leq 5$ between x_n and x_{n+1} . Time t_s and depth h_s when the shock passes x_{n+1} is found by interpolating between x_s^j and x_s^{j-1} where $x_s^{j-1} < x_{n+1} < x_s^j$. The surface profile at any time t_p is found by interpolating from adjacent points (Fig. 3) throughout the grid to determine $h(t_p, x)$ for $0 < x < x_s$. Like-

wise, a flow hydrograph $Q(t)$ for a point x_p is found by computing Q from Eq. 2a for interpolated values of $h(t, x_p)$ for $t > t_s$.

SOLUTION BY RECTANGULAR GRID FINITE DIFFERENCE APPROXIMATION

There are practical advantages to obtaining a solution to Eq. 3 directly, rather than by the system of Eqs. 8–10. Although this has been done by several investigators for plane response to rainfall, the question arises of dealing with the region of discontinuity at the shock. Unfortunately, ordinary finite difference methods cannot follow a moving discontinuity such as a shock. Any scheme which solves Eq. 3 in the region of the shock will necessarily smooth out and diffuse the front. The accuracy with which such a rapid change can be described by finite difference formulations will depend on the order of ap-

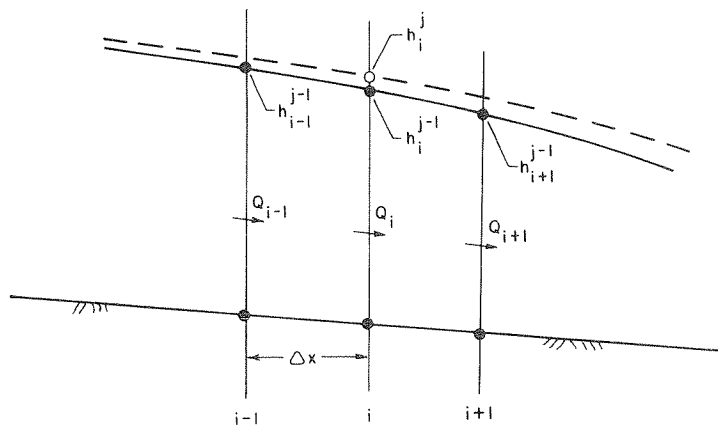


FIG. 4.—DEFINITION SKETCH FOR RECTANGULAR GRID FINITE DIFFERENCE SOLUTION OF KINEMATIC WAVE ADVANCE

proximation, or the number of terms of a Taylor expansion retained in the difference approximation.

Herein, a second-order explicit difference scheme was tested using several methods of defining $(\Delta h^{m+1}/\Delta x)$ to test the finite difference solutions by comparison with the characteristic solution and determining which definition best represented the shock movement. The basic formulation, developed by Kibler and Woolhiser (5) is repeated here, using definitions shown in Fig. 4:

$$h_i^j = h_i^{j-1} - \Delta t \left\{ \frac{\beta}{m+1} \left[\frac{(h_{i+1}^{j-1})^{m+1} - (h_{i-1}^{j-1})^{m+1}}{2\Delta x} \right] - q_i^{j-1} \right\} + \frac{\Delta t^2}{2} \left\{ \frac{\beta}{2} \frac{[(h_i^{j-1})^m + (h_{i+1}^{j-1})^m]}{\Delta x} \left[\frac{\beta}{m+1} \frac{(h_{i+1}^{j-1})^{m+1}}{\Delta x} - \frac{\beta}{m+1} \frac{(h_i^{j-1})^{m+1}}{\Delta x} \right] \right\}$$

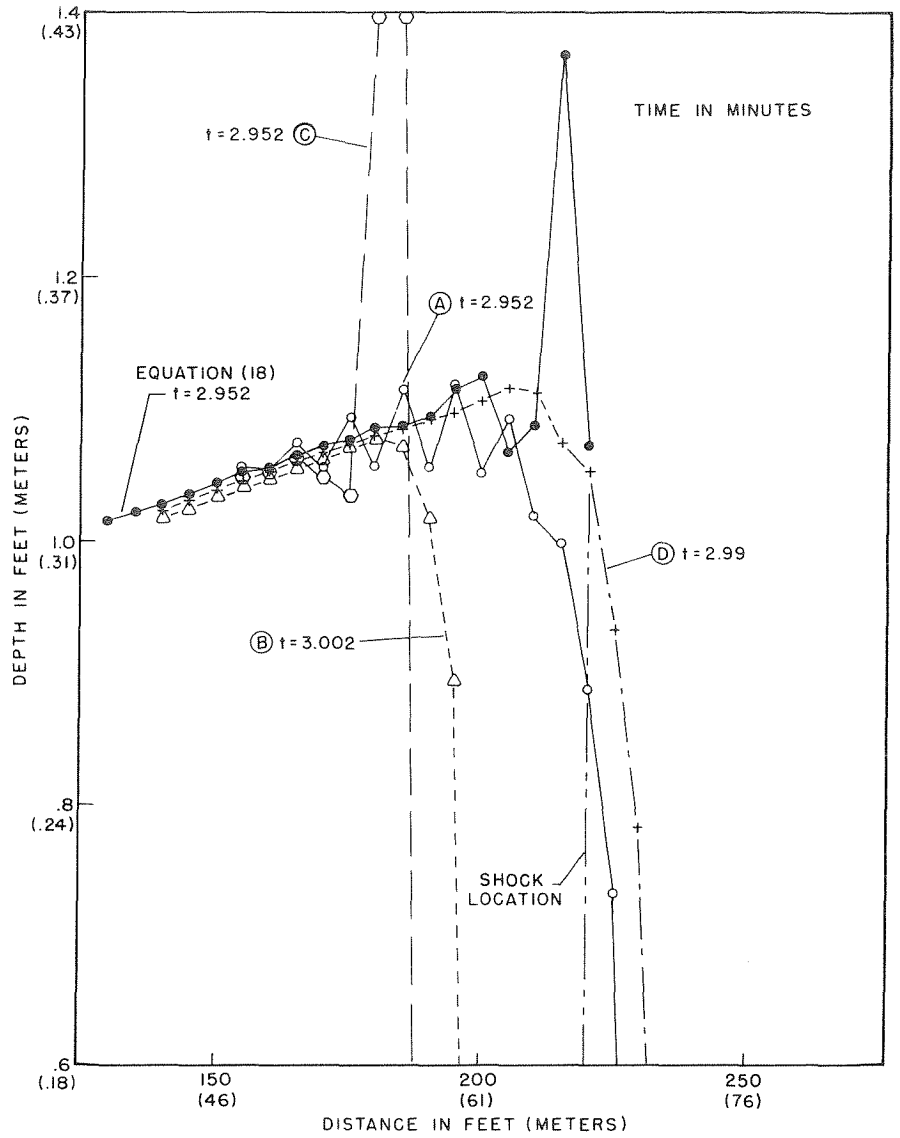


FIG. 5.—EXAMPLES OF CONTINUITY ERROR AND INSTABILITY IN VARIOUS FINITE DIFFERENCE SCHEMES FOR EQ. 18 ACROSS SHOCK

$$\begin{aligned}
 & - \frac{1}{2} (q_{i+1}^{j-1} + q_{i-1}^{j-1}) \Big] \\
 & - \frac{\beta}{2} \frac{[(h_{i-1}^{j-1})^m + (h_{i+1}^{j-1})^m]}{\Delta x} \left[\frac{\beta}{m+1} (h_{i-1}^{j-1})^{m+1} - \frac{\beta}{m+1} (h_{i+1}^{j-1})^{m+1} \right. \\
 & \left. - \frac{1}{2} (q_{i+1}^{j-1} + q_{i-1}^{j-1}) \right] + \frac{(q_i^j - q_{i-1}^{j-1})}{\Delta t} \Big\} \dots\dots\dots (18)
 \end{aligned}$$

Here j represents successive points in time, and i represents the centered point in distance about which the difference equation is constructed. Three adjacent points are required for the second-order scheme. The solution proceeds from $i = 2$ to past the point of farthest front advance.

When these three points encompass a severe change in slope, such as at a shock, the definition of $\Delta h^{m+1}/\Delta x$ becomes critical. Two problems result: one concerns preservation of mass balance, and the other concerns ensuring numerical stability. A brief summary of the numerical results of several of the definitions used will illustrate the problem.

One method tried was to define $\Delta h^{m+1}/\Delta x$ between points i and $i - 1$, or just behind the point i . This proved unstable at the peak of a hydrograph where depth is less at both $i - 1$ and $i + 1$ than at i . The instability is shown by curve A in Fig. 5.

Another definition used a weighted slope between h_{i-1} and a point somewhere between h_i and h_{i+1} . The weighting scheme depended on the change in slope across the three points, or the second difference. The results were stable but conserved mass very poorly, as curve B in Fig. 5 shows.

A method which proved both unstable and erroneous in continuity used definitions of $\Delta(h^{m+1})/\Delta x$ as $(m + 1)h^m (\Delta h)/\Delta x$. Results of this formulation are shown in Fig. 5 as curve C. A peak developed near the shock which travelled and grew.

The best system tested employed a mix of the scheme given as Eq. 18, and a 2-point definition of $\Delta(h^{m+1})/\Delta x$ between i and $i - 1$ for cases where $h_i^{j-1} < h_{i-1}^{j-1}$. Results of this scheme are indicated by curve D in Fig. 5. This method was used in all sample cases reviewed in the next section.

EXPERIMENTAL RESULTS AND ANALYSIS

Experiments reviewed herein consist of a comparison of available field data with computed results from both characteristic and finite difference solutions. The lack of published results from carefully controlled experiments is most evident. Much work needs to be done where infiltration and hydraulic variables are well determined to enable one to study the interaction of surface and porous media flow and to compare theoretical predictions with accurately measured results.

$Q_0 = \text{Constant}$: *Border Irrigation Problem*.—Many interesting approaches to the description of the advance of the front wave under border irrigation have appeared in recent literature. A variety of assumptions have been made regarding both surface and porous media hydraulics. Only a few may be men-

tioned herein. Most have suffered from inadequate data for comparisons.

In one of the earliest analytical approaches, Lewis and Milne (7), by simple continuity, derived an integral convolution expression to describe front movement by assuming constant average surface depth, with infiltration dependent on time since first wetting. Several other authors have followed this pattern, assuming all water surface profiles to be similar, with volume equal to some proportion of upstream (normal) depth times length of front (x_s). Most of these papers are covered by Hart, et al., (3), and some have compared their methods with available published data such as that of Criddle (2). Note that although a few of these papers refer to a kinematic approach, this is often used to mean an assumption of constant depth, or a similarity solution, rather than a true kinematic approach. Surface hydraulics are neglected.

Recently, Kincaid (6) attempted a characteristic solution of the complete equations for unsteady surface flow to describe border irrigation advance. Some difficulty was experienced, however, in the region of the wave front where $\partial h/\partial x$ becomes large. Kincaid found it necessary to adjust predicted wave shapes in the tip region to satisfy continuity. Field comparisons were crippled by the nonuniformity of slope and inconsistency of infiltration data of the plots where comparison was made.

A kinematic shock can describe the border irrigation problem where k is sufficiently large, and where $x_s \leq \xi$, in which ξ is defined by

$$Q_0 \geq \xi f_0 \dots \dots \dots (19)$$

In the limit, as $x_s \rightarrow \xi$, h_s and U_s will approach 0, and the flow becomes steady. Near the limit ξ , however, $f(x, t)$ varies extremely rapidly with x near x_s as shown in Fig. 6.

Wave profiles for a hypothetical border irrigation case computed by characteristic and finite difference methods are shown for comparison in Fig. 7. The numerical diffusion at the shock front in the finite difference method does not seem to increase perceptibly with time, although initial volume balance error because of movement from $n = 1$ to $n = 2$ is carried forward. This error results from initiation of the solution by defining a surface slope between the first grid points. Term k for the example shown is $1.3 L_0$.

Comparison of the kinematic solution and Kincaid's result for one field case is shown in Fig. 8. The results are biased by the fact that slope varied considerably over the reach shown, and infiltration and roughness parameters were estimated by calculations dependent on a power law advance rate assumption. Values for the same plot from different tests were somewhat inconsistent. Although the kinematic solution appears to be better for large times, a fair comparison of the two methods awaits more accurately controlled experiments on more uniform plots. Nevertheless, this comparison indicates that solution of the complete dynamic equations, rather than the more simple kinematic equations, may not be justified for this border irrigation case.

Comparison of the kinematic shock solution with field data from Criddle (2) and the method of Wilke and Smerdon (14) is shown in Fig. 9. As Criddle gave no data on hydraulic roughness, and Wilke and Smerdon used a mean rather than normal depth, it was necessary to estimate roughness.

The infiltration function used in these comparisons is that reported by Criddle (2), based on a ring infiltrometer test. Occurrence of three-dimensional infiltration from such infiltrometers causes inaccuracies, especially at longer times (13), and the difference between predicted and measured advance rates

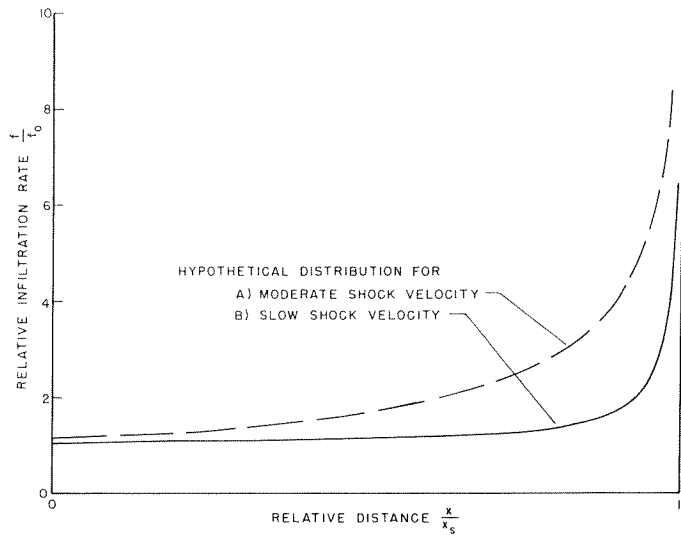


FIG. 6.—EXAMPLE OF SPATIAL DISTRIBUTION OF INFILTRATION RATE AS FUNCTION OF WAVE ADVANCE RATE

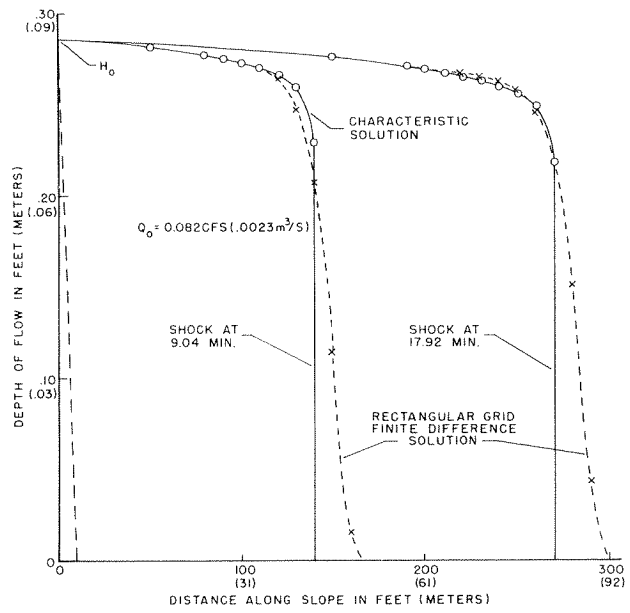


FIG. 7.—COMPARISON OF NUMERICAL SOLUTIONS BY CHARACTERISTIC AND RECTANGULAR GRID METHODS FOR HYPOTHETICAL WAVE ADVANCE PROBLEM

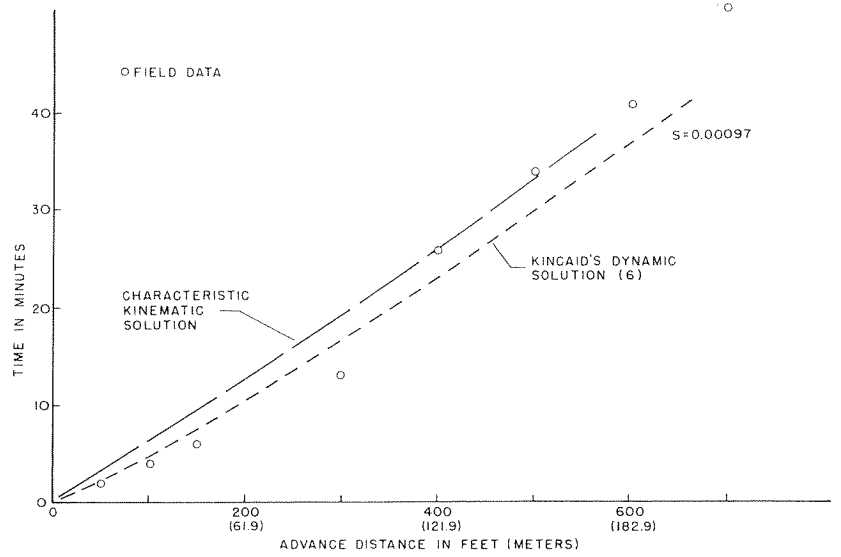


FIG. 8.—COMPARISON OF KINEMATIC AND DYNAMIC WAVE SOLUTIONS TO FIELD DATA FROM KINGAID (6)

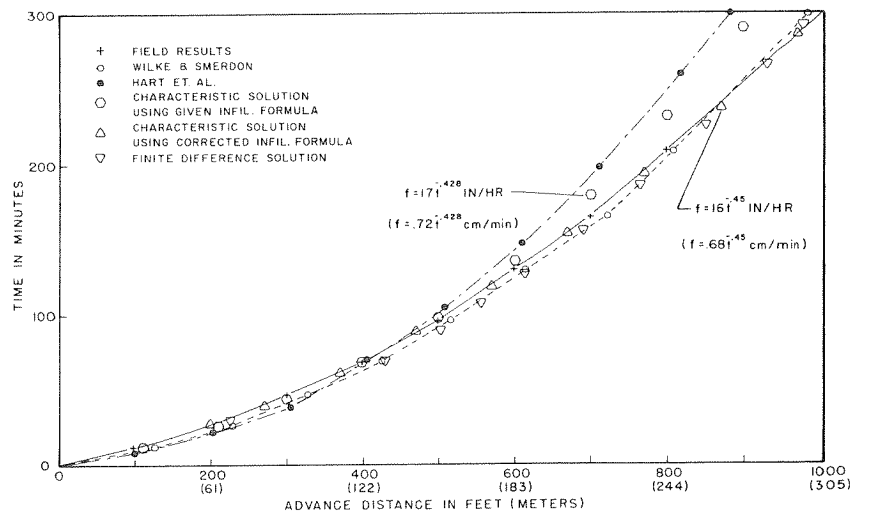


FIG. 9.—COMPARISON OF SEVERAL PREDICTIONS FOR BORDER IRRIGATION ADVANCE FOR DATA FROM CRIDDLE, ET AL., (2), TEST 7

is in the direction of errors from such misestimation of infiltration. Small changes in K and a dramatically improve advance prediction as shown in Fig. 9.

Given that the ring infiltrometer results of Criddle are a somewhat biased estimate of ponded-surface infiltration, the predictions of Wilke and Smerdon, also shown in Fig. 9, must contain a counter-balancing overestimate of front velocity at larger times. Study of their method reveals that, in numerically

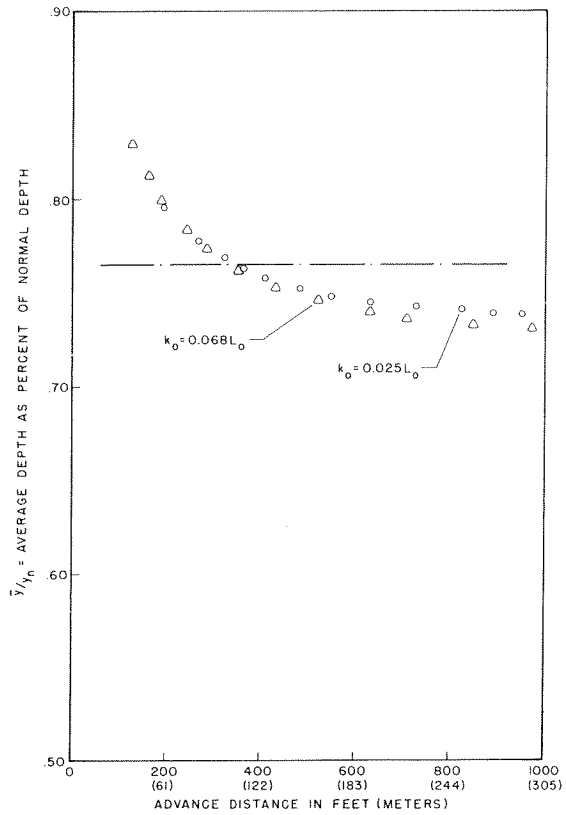


FIG. 10.—AVERAGE DEPTH OF WAVE PROFILE, COMPUTED FOR TWO SAMPLE VALUES OF k_o , AS FUNCTION OF ADVANCE DISTANCE

evaluating the continuity convolution expression of Philip and Farrell (9), nearly linear results over a very limited range of time were extrapolated many times the range in which the results were obtained. The results of Hart, et al. (3) demonstrate the difference between the Wilke-Smerdon predictions by extrapolation and a more accurate evaluation of the same expression.

Surface water profiles obtained by the characteristic kinematic method may be integrated numerically to obtain a value for mean depth of flow. The results, for two values of k_o , are shown in Fig. 10. From these results it

appears that for many cases, the assumption of constant mean depth may be quite justified provided infiltration can be accurately predicted. The data of Fig. 2 predict that, for the example shown with $k_o = 0.025L_o$, the kinematic assumption alone should cause only 3% error, for $x_s \approx 200$ ft (62 m).

The preceding observations suggest an experimental method of determining an infiltration function: with a border irrigation plot of uniform slope and roughness, advance rate data and an accurate measure of upstream (normal) depth could be used with a kinematic model to predict the appropriate infiltration parameters by optimization.

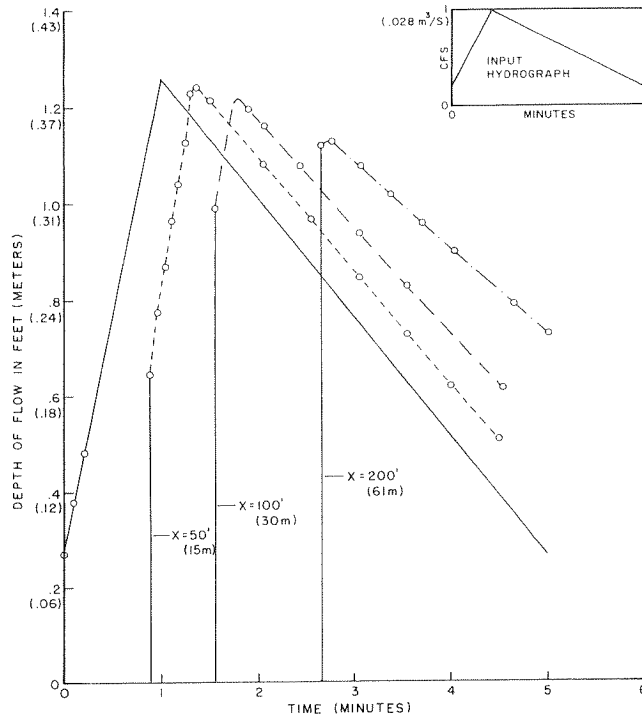


FIG. 11.—SAMPLE RESULTS FOR FLOOD ROUTING ON INITIALLY DRY INFILTRATING BED BY CHARACTERISTIC KINEMATIC METHOD

Both the kinematic finite difference and the characteristic methods appear to represent the data well, given the bias of the infiltration data. The characteristic method begins to demonstrate the effect on solution by segments as used in Eqs. 15—17 of the case where the limit ξ is approached. Some slight instability in computed h_s occurred when $\Delta^2 h / \Delta x^2$ behind the shock became quite large as $d(f(t))/dx$ became large. This difficulty could no doubt be overcome by changing to a fixed Δt and variable Δx scheme at these large times. Here the finite difference method shows practical advantages over the characteristic solution.

Q_o Variable: Routing Ephemeral Flood Waves.—A perhaps more interesting

and unique application of the methods developed above concerns routing of intense local thunderstorm flood waves in dry sand channels such as occur commonly in many parts of the Southwest. In border irrigation, distribution of infiltrated water is the important variable, but for ephemeral flash floods, movement and attenuation of the surface wave is the primary concern. The equations developed above are applicable where channel width is sufficient to approximate R , the hydraulic radius, by h . However, nothing in the technique is altered if the channel is narrow enough so that Eqs. 1a and 2a are used in the development rather than Eqs. 1b and 2b. The algebra, of course, is somewhat more complex.

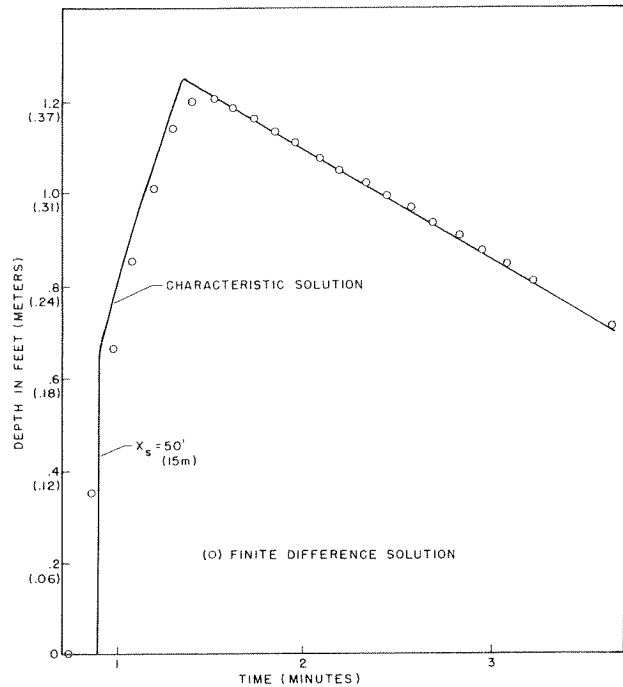


FIG. 12.—COMPARISON OF SOLUTIONS FOR FLOOD WAVE ROUTING IN INFILTRATING CHANNEL BY CHARACTERISTIC AND FINITE DIFFERENCE METHODS

The principal features of shock-type flood wave movement over an infiltrating bed can be shown by the example shown in Fig. 11. The hypothetical input hydrograph is shown in the inset. Shock height grows as the wave moves until the peak is reached because velocity behind the shock exceeds shock velocity; e.g., $\partial Q/\partial x$ for this region is negative. At the same time, the peak flow is decreasing due to infiltration, and the slope of the hydrograph behind the peak is decreasing because $\partial Q/\partial x$ is positive in this region. Infiltration accentuates the increase in slope of the flow profile behind the shock, and also the decrease in slope behind the peak because the loss rate increases at an increasing rate from the rear to the front of the profile.

Downloaded from ascelibrary.org by University of California, San Diego on 06/01/15. Copyright ASCE. For all rights reserved.

The accuracy with which the kinematic wave can be defined by a finite difference solution is indicated by the results shown in Fig. 12. A slight error is shown in predicting peak flow, and some diffusion occurs in the shock front as well, but the difference between finite difference solution and characteristic solution is in the direction of the momentum effects which the kinematic model neglects.

Application of this model to predict flood waves, and comparison with actual events using measured hydraulic and infiltration parameters, is currently being undertaken at the Southwest Watershed Research Center, Tucson, Ariz. Infiltration relationships and channel shape changes will be determined. Flow

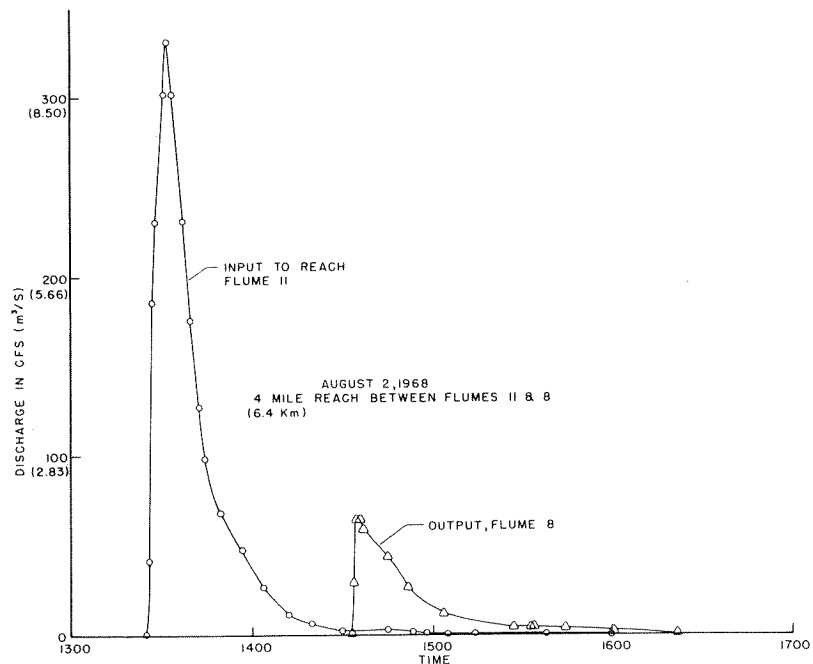


FIG. 13.—SAMPLE OF FLASH FLOOD MOVEMENT AND ATTENUATION IN WALNUT GULCH EXPERIMENTAL WATERSHED, SOUTHEASTERN ARIZONA

measurement structures are still undergoing rating investigations. Fig. 13, however, taken from data on the Walnut Gulch Experimental Watershed, shows how well the kinematic wave characteristics predicted in the example of Fig. 11 are verified by actual hydrographs; obviously infiltration losses are severe. Although rating relations on which this figure is based are somewhat in error, the decay over the reach shown follows quite well those shape change characteristics predicted by the mathematical model.

CONCLUSIONS

A mathematical model of the movement and attenuation of a kinematic shock over an infiltrating plane has been developed, based on a suggestion by Wool-

hiser (1971). The partial differential equations for kinematic wave movement under time-varying and space-varying lateral losses were reduced to two characteristic ordinary differential equations, and combined with a third equation for shock movement. This system of equations was solved numerically, and the model applied to two interesting and important cases of wave flow—border irrigation and ephemeral flood routing.

A rectangular grid finite difference solution of the same partial differential equation was also developed which best modeled the extreme variations at the shock front, by comparison with the characteristic solution.

Results of comparison with available data indicate that for many cases at least, it is unnecessary to solve the complete dynamic equations for this particular unsteady flow case. The constant mean depth used by several previous investigators appears to be a good first approximation; advance rates appear to be much more sensitive to the infiltration function used. The results of Tinney and Bassett (12) indicate at least general guidelines for goodness of the kinematic assumption. The model provides a means for a theoretical description of border irrigation hydraulics where, in the past, gross assumptions were used for surface profile shape. Moreover, it provides a promising means for study of ephemeral flood routing and attenuation from channel losses. Further field research will better establish the accuracy of the model as a descriptive and predictive tool.

ACKNOWLEDGMENT

This paper is a contribution of the Soil and Water Conservation Research Division, Agricultural Research Service, USDA, in cooperation with the Arizona Agricultural Experiment Station, Tucson, Ariz.

APPENDIX I.—REFERENCES

1. Chen, C. L., "Surface Irrigation Using Kinematic-Wave Method," *Journal of the Irrigation and Drainage Division*, ASCE, Vol. 96, No. IR1, Proc. Paper 7134, March, 1970, pp. 39-46.
2. Criddle, W. D., et al., "Methods for Evaluating Irrigation Systems," *Agricultural Handbook No. 82*, Soil Conservation Service, U.S. Dept. of Agric., Washington, D.C., 1956.
3. Hart, W. E., Bassett, D. L., and Strelkoff, T., "Surface Irrigation Hydraulics—Kinematics," *Journal of the Irrigation and Drainage Division*, ASCE, Vol. 94, No. IR4, Proc. Paper 6284, December, 1968, pp. 419-440.
4. Henderson, F. M., "Flood Waves in Prismatic Channels," *Journal of the Hydraulics Division*, ASCE, Vol. 89, No. HY4, Proc. Paper 3568, July, 1963, pp. 39-67.
5. Kibler, D. F., and Woolhiser, D. A., "The Kinematic Cascade as a Hydrologic Model," *Hydrology Paper No. 39*, Colorado State Univ., Ft. Collins, Colo., March, 1970.
6. Kincaid, D. C., "Hydrodynamics of Border Irrigation," dissertation presented to Colorado State Univ., Ft. Collins, Colo., in August, 1970, in partial fulfillment of the requirements for a degree of Doctor of Philosophy.
7. Lewis, M. R., and Milne, W. E., "Analysis of Border Irrigation," *Agricultural Engineering*, Vol. 19, June, 1938, pp. 267-272.
8. Lighthill, M. J., and Whitham, G. B., "On Kinematic Waves. I. Flood Movement in Long Rivers," *Proceedings of the Royal Society of London, Series A*, Vol. 229, 1955, pp. 281-316.

9. Philip, J. R., and Farrell, D. A., "General Solution of the Infiltration-Advance Problem in Irrigation Hydraulics," *Journal of Geophysical Research*, Vol. 69, No. 4, February 15, 1964, pp. 621-631.
10. Smith, R. E. "The Infiltration Envelope; Results from a Theoretical Infiltrometer," Presented at American Geophysical Union Winter 1971 Meeting, San Francisco, Calif.
11. Smith, R. E., and Woolhiser, D. A., "Mathematical Simulation of Infiltrating Watersheds," Hydrology Paper No. 47, Colorado State Univ., Ft. Collins, Colo., January, 1971.
12. Tinney, E. R., and Bassett, D. L., "Terminal Shape of a Shallow Liquid Front," *Journal of the Hydraulics Division*, ASCE, Vol. 87, No. HY5, Proc. Paper 2934, Sept., 1961, pp. 117-133.
13. Wei, Chi-Yuan, and Jeppson, R. W., "Finite Difference Solutions of Axisymmetric Infiltration through Partially Saturated Porous Media," *Report No. PRWG59c-6*, Utah Water Research Laboratory, Logan, Utah, April, 1971.
14. Wilke, Otto, and Smerdon, E. T., "A solution of the Irrigation Advance Problem," *Journal of the Irrigation and Drainage Division*, ASCE, Vol. 91, No. IR3, Proc. Paper 4471, September, 1965, pp. 23-34.
15. Woolhiser, D. A., discussion of "Surface Irrigation Using Kinematic Wave Method," by Cheng-lung Chen, *Journal of the Irrigation and Drainage Division*, ASCE, Vol. 96, No. IR4, Proc. Paper 7134, Dec., 1970, pp. 498-500.
16. Woolhiser, D. A., and Liggett, J. A., "Unsteady, One-Dimensional Flow Over a Plane—The Rising Hydrograph," *Water Resources Research*, Vol. 3, No. 3, 1967, pp. 753-771.

APPENDIX II.—NOTATION

The following symbols are used in this paper:

- A = channel cross-sectional area;
- a = exponent of time in infiltration equation;
- C_1 = laminar resistance coefficient;
- C_t = turbulent resistance coefficient;
- F_o = Froude number;
- f = infiltration rate;
- $f_o = f$ at $t \rightarrow \infty$;
- H_o = normal depth of water;
- h = depth of water;
- h_c = depth of water at intermediate point (Fig. 3);
- h_s = depth of shock;
- i = node number in x direction finite difference grid;
- j = node number in t direction finite difference grid;
- K = time coefficient in infiltration equation;
- $k = S_o L_o / H_o F^2$ = Liggett and Woolhiser parameter for goodness of kinematic assumption;
- $k_o = S_o L_o / H_o$ = parameter from Tinney and Bassett;
- L_o = normalizing (plane) length;
- m = exponent to depth in friction relation;
- n = node number in x direction on characteristic grid;
- p = wetted perimeter;
- Q = discharge;
- Q_o = constant upstream input for border irrigation;
- Q_s = discharge immediately behind shock;

- q = local inflow or outflow rate from surface flow;
 S_o = bed slope;
 t = time;
 t_c = time defined at an intermediate point on characteristic grid (Fig. 3);
 t_s = time for shock to reach point x ;
 U_s = shock velocity;
 u = local velocity;
 x = distance along plane;
 x_s = distance to shock at time t_s ;
 α = coefficient in stage-discharge relation;
 $\beta = \alpha(m + 1)$;
 $\xi = Q_o/f_o$; and
 $\tau = t - t_s$ = time since initial wetting.

8979 BORDER IRRIGATION ADVANCE AND EPHEMERAL FLOOD WAVES

KEY WORDS: **Floods; Hydrology; Infiltration; Irrigation; Kinematics; Mathematical models; Routing; Transmission loss**

ABSTRACT: Movement and modification of an advancing front on an initially dry infiltrating surface is modelled mathematically by a kinematic description of surface flow and a kinematic shock. Criteria for the goodness of approximation are presented, and the model is shown to describe two common hydraulic problems; border irrigation advance and dry channel flood wave movement. Two numerical methods for solution of the equations involved are developed and compared. Results from the kinematic model are compared with published data and other methods of predicting border irrigation advance. Sensitivity of advance rate to the infiltration relations is demonstrated, and a constant mean depth is shown to be a reasonable assumption as a first approximation. The model may also be used to route floods through a dry infiltrating channel, and correspondence of properties of measured floods with kinematic shock waves is demonstrated.

REFERENCE: Smith, Roger E., "Border Irrigation Advance and Ephemeral Flood Waves," *Journal of the Irrigation and Drainage Division*, ASCE, Vol. 98, No. IR2, Proc. Paper 8979, June, 1972, pp. 289-307